Inorganic Chemistry

Article

pubs.acs.org/IC

Computational Studies of the Metal-Binding Site of the Wild-Type and the H46R Mutant of the Copper, Zinc Superoxide Dismutase

Raúl Mera-Adasme,*[,†,‡] Fernando Mendizábal,[†,¶] Mauricio Gonzalez,[§] Sebastián Miranda-Rojas,[†,⊥] Claudio Olea-Azar,[⊥] and Dage Sundholm[‡]

[†]Department of Chemistry, Faculty of Sciences, Universidad de Chile, Santiago, Chile

[‡]Department of Chemistry, P.O. Box 55 (A.I. Virtanens plats 1), FIN-00014 University of Helsinki, Finland

[¶]Center for the Development of Nanoscience and Nanotechnology, CEDENNA, Santiago, Chile

[§]Instituto de Nutricion y Tecnología de los Alimentos (INTA), Universidad de Chile, Santiago, Chile

[⊥]Department of Analytic and Inorganic Chemistry, Faculty of Chemical and Pharmaceutical Sciences, Universidad de Chile, Santiago, Chile

Supporting Information

ABSTRACT: Impairment of the Zn(II)-binding site of the copper, zinc superoxide dismutase (CuZnSOD) protein is involved in a number of hypotheses and explanations for the still unknown toxic gain of function mutant varieties of CuZnSOD that are associated with familial forms of amyotrophic lateral sclerosis (ALS). In this work, computational chemistry methods have been used for studying models of the metal-binding site of the ALS-linked H46R mutant of CuZnSOD and of the wild-type variety of the enzyme. By comparing the energy and electronic structure of these models, a plausible explanation for the effect of the H46R mutation on the zinc site is obtained. The computational study clarifies the role of the D124 and D125 residues for keeping the structural integrity of the Zn(II)-binding site, which was known to exist but its mechanism has not been explained. Earlier results suggest that the explanation for the impairment of the Zn(II)-site proposed in this work may be useful for understanding the mechanism of action of the ALS-linked mutations in CuZnSOD in general.

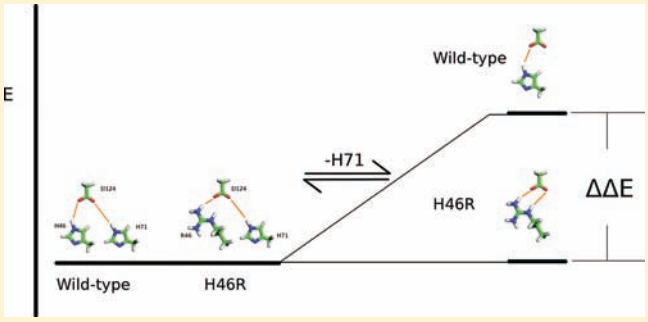

1. INTRODUCTION

Amyotrophic lateral sclerosis (ALS) is a fatal neurodegenerative disease affecting motor neurons. It produces a progressive paralysis that ends in respiratory failure, causing the death of the patient in about 2−5 years from the diagnosis. Among the variants of ALS, it is possible to distinguish between the ones where the patients have a family history of the disease and the ones for which no familial link can be found. The former variants are referred to as familial ALS, or fALS, which accounts for about 10% of the cases, and the latter one is known as sporadic ALS or sALS. The pathogenesis of both forms is poorly understood.[1] Thus, no effective cure or treatment for the disease is currently available. Riluzole, the only FDA-approved drug for the treatment of the disease, extends the life of the patients by about two to three months.[2]

Alterations of the protein structure have been shown to be characteristic for ALS as they also are for other neurodegenerative diseases. Mutations in the Cu, Zn superoxide dismutase (CuZnSOD), occurring practically along the whole sequence of this protein have been shown to produce different forms of fALS.[3,4] Such mutations, considered together, account for about 20% of all fALS cases, and thus, about 2% of all ALS cases. CuZnSOD-linked fALS and animal models for the disease based on CuZnSOD mutations have been widely studied during the last few decades. This has been done in the hope that the knowledge obtained from studies of SOD-linked fALS is useful for understanding and treating sALS.[5,6]

1.1. CuZnSOD. CuZnSOD is the main quencher of the superoxide radical in mammals. The mammalian protein forms a homodimer of 32 kDa, where each monomer contains an active site. The active site contains a copper ion as the catalytic center. The copper ion fluctuates between the Cu(I) and Cu(II) oxidation states along the catalytic cycle of the protein. Close to the copper center in the active site, there is a zinc center in each monomer. The Zn(II) center, which is not exposed to solvent according to the crystallographic structures, has been shown to be important for the structural integrity of the protein.[7] The zinc site also participates, at least indirectly, in the catalytic process.[8]

When a monomer of the protein is in the oxidized state, the Cu(II) center is pentacoordinated with a distorted square-pyramidal geometry. Its first four ligands are histidine residues: H46, H48, H63, and H120. The fifth ligand is a weakly bound

Received: November 9, 2011
Published: April 30, 2012

   dx.doi.org/10.1021/ic202416d | *Inorg. Chem.* 2012, 51, 5561−5568

water molecule.[9] The zinc ion in the oxidized protein is tetracoordinated with a distorted tetrahedral geometry. All the ligands of Zn(II) are aminoacidic residues, consisting of one deprotonated aspartic acid residue (D83) and three histidine residues, H63, H71, and H80. The H63 residue is thus a ligand to both Cu(II) and Zn(II). The H63 residue is negatively charged and bonded with its ε2 nitrogen to Cu(II) and with its δ1 nitrogen to Zn(II). The doubly deprotonated histidine forms what is called an imidazolate bridge between the two metal centers. In addition, there is a secondary bridge, formed by the deprotonated aspartic acid residue D124. D124 forms hydrogen bonds to H46, which is one of the copper ligands, and to H71, which is ligated to Zn(II).[10] The metal site of the oxidized form of CuZnSOD is shown schematically in Figure 1.

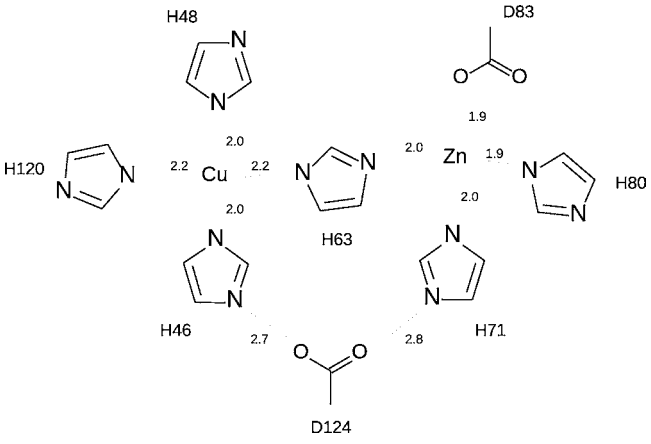

Figure 1. Schematic view of the spacial arrangement of the metal-binding site of the oxidized form of CuZnSOD, according to crystallographic data.[10] The D83 and D124 residues are shown from the β-carbons. For histidines, β-carbons were omitted for simplicity. Distances are given in Ångströms.

The molecular structures of the reduced and oxidized protein have a few differences. In the reduced state, the imidazolate bridge is broken. The bridging residue, H63, is protonated at its ε2 nitrogen and bends away from the Cu(I) center, thus becoming exclusively a Zn(II) ligand. The water ligand disappears from the copper center. The secondary bridge is intact in the reduced form, according to the crystallographic structures.[11,12]

The post-translational modifications of CuZnSOD include insertion of both metal atoms, and formation of a disulfide bond between residues C57 and C146. The insertion of Zn(II) is thought to occur earlier, while the formation of the disulfide bond and the insertion of copper probably occur almost simultaneously.[13,14] It has been shown that the copper chaperone for SOD (CCS), which inserts the copper ion to CuZnSOD, is also responsible for the formation of the disulfide bond.[14] The process that inserts zinc in superoxide dismutase is unelucidated. Because of the extremely low Zn(II) concentration in cells,[15] it is possible that an unknown factor could participate in the process.[13] Considering the large amount of different zinc proteins, it is unlikely that there would be a specific factor for each of them.[16] Considering all this, it has been suggested that the metallothioneines (MT) are responsible for delivering zinc to the Zn-containing proteins without any direct interaction with the target proteins.[13,17]

1.2. CuZnSOD and ALS. A large variety of mutations in CuZnSOD, distributed along the whole sequence, are known to cause forms of fALS. Regarding the relationship between CuZnSOD mutations and fALS, it is known that the reason for the SOD-linked fALS is not a loss of the catalytic function of the enzyme. This has been proven by various observations, including that coexpression of wild-type (WT) CuZnSOD in mice expressing a fALS-linked CuZnSOD mutants still develop an ALS-like syndrome, whereas mice whose expression of CuZnSOD have been ablated do not develop the syndrome. It is thus said that the fALS syndrome produced by mutants of CuZnSOD arises from a gain of a pathological function from this protein due to the mutations,[5,18] whereas the function gain of ALS-associated CuZnSOD mutants is currently unknown.

The generally accepted explanation for the toxicity of CuZnSOD is the formation of toxic aggregates of the enzyme.[1,6,13,18,19] The aggregates can cause cellular insult in different ways, including perturbation of the cytoskeleton and the cellular endoplasmatic-reticle-associated degradation pathway for misfolded proteins.[19] One of the possible reasons for the aggregation of CuZnSOD is the loss of the Zn(II) ion from the protein. It is known that the Zn(II) ion plays an important role in the folding process, and that the loss of zinc is associated with increased aggregation of CuZnSOD.[20−22] Although the zinc affinity in mutants with the aminoacidic substitution occurring far away from the active site was controversial,[7,23] it was later suggested that such mutations could cause structural distortions of the active site, facilitating structural damage that would lead to loss of metal affinities.[24,25] It has also been suggested that a distortion of the zinc loop (residues 50−83), which can be caused by the detachment of only the histidine 71 ligand from the Zn(II) center, can lead to aggregation of CuZnSOD.[24,26]

1.3. Zinc and ALS. Alterations related to Zn(II) could be the main cause of the syndrome caused by the CuZnSOD-linked forms of fALS. By considering the variety of functions of Zn(II),[16] Smith and Lee (2007) proposed that alterations on the labile zinc levels of the neurons or glia might affect all the processes that have been linked to ALS. Therefore, they suggested that dyshomeostasis of Zn(II) could be responsible for ALS.[27] This notion was supported by a study by Kim et al. (2009),[28] who found elevated levels of labile zinc in neurons of animals expressing the fALS-linked G93A mutation, which occurs far from the metal-binding site. In the study, they found a correlation between the levels of labile zinc and the progression of the disease. The lifespan of the mice was found to be extended by intraperitoneal treatment with a cell-permeant zinc chelator. Later, it was found by Lelie et al. (2011) that G93A and two other mutants, G37R and H46R, produce an increase of zinc in the white matter, which does not occur for mice expressing WT human CuZnSOD.[29]

The Zn(II) binding to CuZnSOD and its alterations in fALS-linked mutants are thus involved in different hypotheses that could account for the pathogenesis of CuZnSOD-linked fALS or even sALS. Therefore, it is important to investigate how zinc binds to CuZnSOD and how protein mutations can affect the Zn(II) affinity. Quantum chemical calculations at the density-functional theory (DFT) level have been previously employed in studies on the metal-binding site of CuZnSOD.[9,30,31] The aim of the earlier studies was to understand the physiological, catalytic role of CuZnSOD, rather than the pathological characteristics of the ALS-linked mutants.

In this work, the molecular structure of the CuZnSOD binding site is studied using quantum-chemical methods. Metal-binding site models consisting of about 97 atoms have been

dx.doi.org/10.1021/ic202416d | Inorg. Chem. 2012, 51, 5561−5568

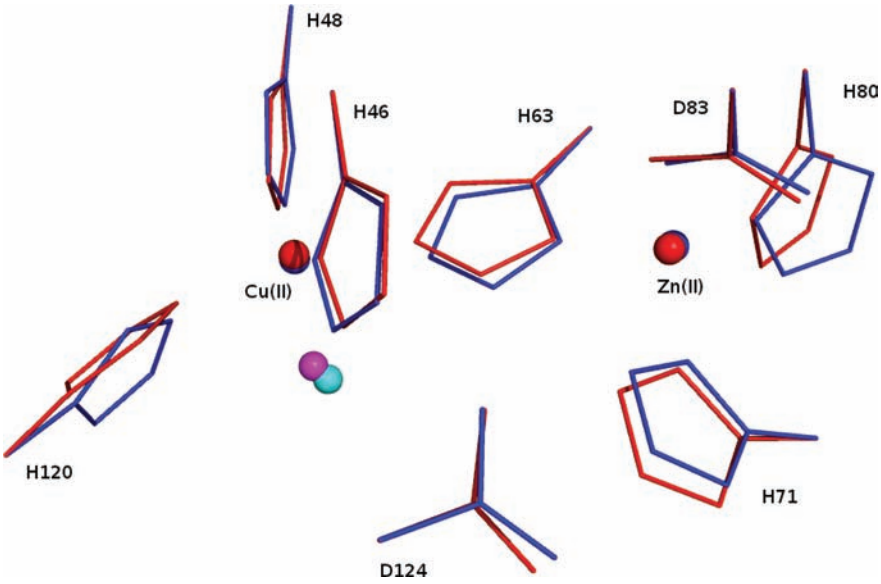

Figure 2. Comparison between the crystallographic structure of the metal-binding site of WT-CuZnSOD (blue) and the calculated one (red). The water molecules coordinated to the copper are shown in cyan and magenta for the experimental and calculated structures, respectively.

generated using experimental crystallographic data. The ALS-linked mutation effects on the electronic structure of the metal-binding site have been studied at the DFT level. The energy and charge distribution have been investigated for the oxidized protein models with the copper ion formally in Cu(II) form. The mutation effects on the molecular structure of the metal-binding site was investigated by comparing calculations on the WT and the fALS-linked mutant variety of CuZnSOD H46R. The H46R mutant lacks enzymatic activity and has a greatly impaired metal binding.[23] The crystal structure shows that the mutant can be isolated with Zn(II) content.[32] The H46R mutant is convenient for quantum mechanical studies because the aminoacidic substitution occurs in the metal site, thus making it is feasible to capture the effects of the mutation in a reduced model.

2. COMPUTATIONAL DETAILS

2.1. General Computational Methods. The BP86 density functional[33,34] with the dispersion correction developed by Grimme in the 2006 version[35] and the RI approximation[36] were used in most calculations. For comparison, some calculations were also performed using other density functionals such as BLYP,[33,37] PW91,[38] TPSS,[39] mPW1PW,[40] and B3LYP.[37,41−43] For the calculations employing hybrid functionals, the COSX approximation was used.[44] Grimme's dispersion correction was used for those functionals for which it was available,[35] and its use is indicated by appending "-D" to the acronym of the density functional. The calculations were performed with the def2-SVP and def2-TZVPP basis sets.[45] All calculations were performed with the ORCA[46,47] program package using COSMO[48,49] to model the environmental effects. A dielectric constant of 4 was used.[30] The NBO set of tools and the NBO-based fopBO bond order indicator were also employed.[50−53]

2.2. Reduced Models. The systems were built based on the crystallographic structure for the WT CuZnSOD with a resolution of 1.65 Å.[10] A crystallographic structure for the H46R mutant form has been reported,[32] but we chose to use the wild-type structure also for the mutants and add the mutation with a molecular editor. The aim of this procedure was to investigate how the aminoacidic substitution affects the native WT structure.

The reduced models were constructed by considering only the metal ions and the aminoacidic residues directly bonded to them. The secondary bridge, which is not a direct ligand of any of the metals but has been shown to be important for the zinc site integrity, was also included.[8] The side chain of all residues were cut at the bond between the α and β carbons. The α carbons were replaced by hydrogens.

Three reduced models were built based on the crystallographic structure for the H46R mutant variety of CuZnSOD.[32] They included all residues bound to the metals in the WT structure, except for residue H71. The D124 and D125 residues were also included in the models. All residues except D124 and D125 were considered up to the β-carbon. Part of the backbone of the D124 residue and the complete D125 residue were included. The C_α−N bond of D124 was cut and the nitrogen atom was replaced with an hydrogen. The entire residue L126 was replaced with an amine group.

2.3. Basis Sets. Because of the large size of the systems (90 atoms for the smallest models), we used combinations of Karlsruhe of basis sets. The employed basis sets are denoted I to IV.

I. Consists of def2-TZVPP for the metal atoms and def2-SVP for the rest. It was used for geometry optimizations.
II. Consists of def2-TZVPP for metal atoms and all the atoms directly involved in the studied interactions (i.e., metal−ligand interactions and the two hydrogen bonds in the systems) and def2-SVP for all other atoms. It was used in the NBO-related analyses.
III. Consists of def2-TZVPP for all atoms except carbons, for which def2-SVP was used. Basis set III was used in single-point energy calculations.
IV. Consists of def2-TZVPP for all atoms and was used to check the basis-set convergence.

2.4. Geometry Optimizations. The molecular structure optimizations were carried out with the basis set I. For the models based on the WT-crystallographic structure, the position of the β-carbon of each residue was kept fixed in the crystallographic position, in order to mimic the spatial restraints imposed to the metal site by the protein.

For the models based on the H46R mutant crystallographic structure, the position of the β-carbons were also fixed, except for the D124 and D125 residues. For D124, the position of the α-carbon was kept fixed during the optimizations. For D125, the position of the nitrogen atom of the amine replacing L126 was kept fixed.

3. RESULTS AND DISCUSSION

3.1. Geometries. The molecular structures for the oxidized models of the metal-binding sites of CuZnSOD were optimized

dx.doi.org/10.1021/ic202416d | Inorg. Chem. 2012, 51, 5561−5568

at the BP86 level using the basis sets I. The initial structure was based on the crystallographic structure determined by 1CBJ.[10] The optimized structure for the model corresponding to the WT protein remained very similar to the crystallographic structure, utilized as a reference (Figure 2). The root-mean square deviation (rmsd) between the two structures was 0.37 Å. The structural features of the crystallographic site[10,54] are conserved in the optimized geometry, suggesting that the optimized structures are appropriate for the subsequent analyses of the energetics and the electronic structure of the metal-binding site.

3.2. Energetics Analyses. From the structural data for the mutant H46R,[32] it is reasonable to assume that the loss of the residue H71 from the zinc coordination sphere is related to the loss of the metal itself from the site, probably as a first step to the zinc loss. In the crystallographic structure, the loss of the H71 ligand from the zinc site causes considerable structural changes in the metal center. In the absence of H71, the zinc atom is exposed to solvent and the zinc loop lacks a stable structure.[32] Thus, the aim of the present study is to understand the reasons for the loss of H71 from zinc-binding site of the mutant. In this section, we study the effect of the H46R mutation of CuZnSOD on the energetics of the H71 dissociation.

To validate our computational approach, we calculated the binding energy difference ($\Delta\Delta E_{binding}$) for the residue H71 between the WT-metal site and the H46R mutant metal site. The $\Delta\Delta E_{binding}$ was obtained using the following procedure: the total energy was calculated using the optimized geometry of the WT metal-site model (E(WT)). The residue H71 was removed from the model, and the structure was reoptimized. The E(WT,Incomplete) energy was calculated for the optimized incomplete model. A similar procedure was used for the mutant models, yielding E(H46R) and E(H46R,Incomplete). Finally, the $\Delta\Delta E_{binding}$ was obtained as

$$\Delta\Delta E_{binding} = (E(\mathrm{WT}) - E(\mathrm{WT, Incomplete})) - (E(\mathrm{H46R}) - E(\mathrm{H46R, Incomplete})) \quad (1)$$

A negative $\Delta\Delta E_{binding}$ value indicates that H71 has a larger binding energy for the WT-model than for the mutant. Since the copper binding is impaired in the H46R mutant,[32] we have determined $\Delta\Delta E_{binding}$ for models with and without copper.

Crystallographic data suggests that the binding of H71 to the Zn(II) site of CuZnSOD is perturbed in the H46R mutant as compared to the WT form. H71 is not observed at the metal site of the mutant crystallographic structure, but seems to appear in all the crystallographic structures of the wild-type form.[10,11,32] If our model correctly reproduces the energetics of the zinc site of CuZnSOD, negative $\Delta\Delta E_{binding}$ values should be obtained.

The $\Delta\Delta E_{binding}$ values given in Figure 3 are all negative, in agreement with the experimental data. For the models without copper, largely the same energies are obtained with all basis sets. Energies calculated using basis sets II and III, which were used for analyses, show good agreement with the reference set IV. For the structures containing copper, the $\Delta\Delta E_{binding}$ value is more sensitive to the size of the basis set. The calculations using basis set IV did not converge for the models containing copper.

The $\Delta\Delta E_{binding}$ values for the residue H71 obtained with basis set III are −10.0 kcal/mol and −11.6 kcal/mol for the systems with and without copper, respectively. The negative

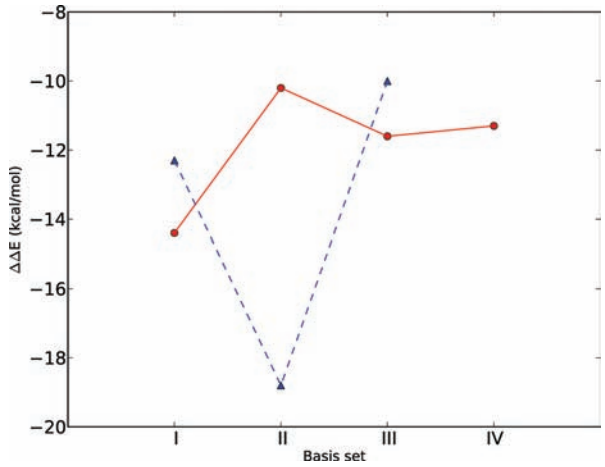

Figure 3. The $\Delta\Delta E_{binding}$ (in kcal/mol) for H71 obatined between models for WT and H46R CuZnSOD, using different basis sets. Results for systems with (blue triangles and dash line) and without copper (red circles and solid line) are shown.

$\Delta\Delta E_{binding}$ values indicate that the H71 interaction with Zn(II) is stronger for the WT form than for the H46R mutant. The $\Delta\Delta E_{binding}$ values were also calculated with a variety of other density functionals. Single-point energy calculations using the BP86-optimized structures were performed employing GGA, meta-GGA, and hybrid functionals. Previous studies have shown that the GGA and hybrid functionals employed here provide accurate descriptions of Zn−ligand interactions and hydrogen bonds (an hydrogen bond is present between H71 and D124).[55−57] The energies were calculated not only for structures with and without copper, but also for hybrid models in which the WT structure contains copper and the H46R mutant structure does not. The reduced affinity of the H46R mutant CuZnSOD for copper makes the hybrid models biologically relevant.

The $\Delta\Delta E_{binding}$ values obtained with different density functionals are listed in Table 1. All the energies are negative and largely independent of the employed functional.

Table 1. The Obtained Difference in the Interaction Energy for H71 between WT and H46R Mutant Structures ($\Delta\Delta E_{binding}$, in kcal/mol)[a]

density functional	$\Delta\Delta E_{binding}$(Cu)	$\Delta\Delta E_{binding}$(non-Cu)	$\Delta\Delta E_{binding}$(Cu−non-Cu)
BP86-D	−10.0	−11.6	−8.7
B3LYP-D		−10.7	−10.1
PW91	−7.4	−13.9	−9.5
BLYP-D	−10.2	−11.5	−8.5
TPSS-D	−7.6	−13.1	−8.5
mPW1PW		−7.6	

[a]The values obtained using different density functionals are given for structures containing Cu(II), without Cu(II) and with only the WT form containing Cu(II), respectively. The missing values correspond to calculations that did not converge.

The reliability of the calculated $\Delta\Delta E_{binding}$ values was assessed using an experimental control. As such control, we performed similar calculations for the histidine 80 (H80), which is a zinc ligand in both WT and H46R mutant crystallographic structures of CuZnSOD.[10,11,32] Since the coordination of H80 is not affected by the H46R mutation,

dx.doi.org/10.1021/ic202416d | Inorg. Chem. 2012, 51, 5561−5568

the $\Delta\Delta E_{binding}$ values for H80 are expected to be small if the computational methodology produces accurate energies. For the copper-containing models, the models without Cu, and for the models for which only the WT-structure contained copper, calculations using the BP86 density functional very small $\Delta\Delta E_{binding}$ values of 1 kcal/mol, −1.3 kcal/mol and −1.9 kcal/mol, respectively. The small magnitude of the $\Delta\Delta E_{binding}$ values for the control residue H80 is consistent with the crystallographic information and suggests that the employed DFT calculations are accurate for these systems.

The reorganization contribution to $\Delta\Delta E_{binding}$ was assessed using a similar computation procedure as used for calculating $\Delta\Delta E_{binding}$, but without allowing the structures to relax after removal of H71. Thus, the values do not include the reorganization contribution. For the more biologically relevant noncopper and mixed systems, the results in Table 2 show that

Table 2. The Differences in the Interaction Energy ($\Delta\Delta E_{binding}$, in kcal/mol) for H71 between the WT and H46R Mutant Structures[a]

calculation/system	$\Delta\Delta E_{binding}$(Cu)	$\Delta\Delta E_{binding}$ (kcal/mol)	$\Delta\Delta E_{binding}$ (Cu−non-Cu)
nonopt	−4.7	1.1	4.6
steric	29.0	45.3	106.2

[a]The energies include values obtained without optimizing the structures after H71 removal (non-opt) and the energy contributions due to steric effects (steric).

the $\Delta\Delta E_{binding}$ values in Table 1 are due to reorganization of the metal site after removal of the H71 residue and not due to destabilization of the metal site in the H46R mutant.

In the H46R mutant, the histidine is replaced by an arginine, which is larger. The mutation might therefore lead to an increase in the energy due to steric effects, which can be assessed using the NBO program.[52] The steric contributions to the $\Delta\Delta E_{binding}$ values were obtained using the optimized structures and basis set II, which was the largest feasible one in the NBO calculations. The values for the steric contributions, listed in Table 2, are large and positive, suggesting that the reduced affinity of H71 to the metal in the H46R mutant is not due to steric effects.

The present calculations show that the binding energy of the H71 residue is less favorable in the H46R mutant than in the WT form, in agreement with the crystallographic information. Our studies of the nature of the reduced interaction energy for H71 in the H46R mutant suggest that the smaller interaction energy is due to stabilization of the metal site of the mutant in the absence of the H71 residue. The stabilization decreases the energy for the removal of the histidine 71.

3.3. Density Matrices Analyses. The experimental data that link the H46R mutation of CuZnSOD to the reduced affinity of the metal site for the residue H71 have been reproduced by using energy analyses. Although the results suggest reasons for the reduced affinity, studies of the electronic structure of the systems are needed for obtaining a detailed description of the impairment of the interaction of the H46R metal site with the H71 residue. The analyses of the density matrices for the WT and mutant metal sites of CuZnSOD are used to estimate the partial charges of the metal ions and of the residues of the mutant and WT metal sites, as well as for determining bond orders for selected interactions. The analyses were performed with the NBO program and basis set II. Because of the poor results obtained in the energetic analysis from the copper-containing systems, the density matrix analyses have been restricted to the systems without copper.

3.3.1. Natural Population Analyses. A schematic representation of the metal site of the WT-CuZnSOD was given in Figure 1. A scheme for our model of the metal site of the H46R mutant is shown in Figure 4. The residues are grouped in the

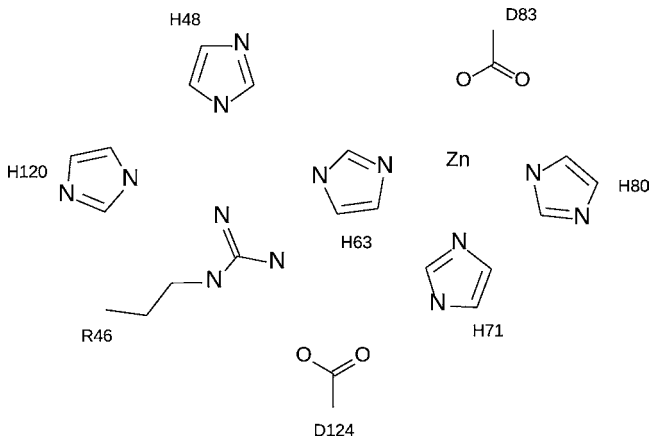

Figure 4. Schematic view of the spatial arrangement of the model for the metal-binding site of the H46R variety of CuZnSOD without the copper ion. Hydrogens, as well as histidine β-carbons, are omitted for simplicity.

following categories: The "Zn-site", which comprises the Zn(II) ion and its ligands, H63, H71, H80, D83 and the "Cu-site" which comprises the exclusive Cu ligands in the copper-containing protein H46 or R46, H48, H120 and the water molecule were found ligated to copper in the crystallographic structure of the protein.[10]

The natural charges or partial charges obtained with the natural population analysis (NPA) procedure for the WT and H46R models are shown in Table 3. In the molecular structures

Table 3. Natural Charges for the Copper-Free Models of the WT-CuZnSOD and its H46R Mutant

residue or fragment	wild-type (e)	H46R (e)
Zn(II)	1.61	1.61
D124	−0.77	−0.78
H63	0.01	0.02
H71	0.04	−0.08
H80	0.05	0.08
D83	−0.85	−0.84
H48	−0.02	0.06
H/R46	0.01	0.82
H120	0.06	0.02
H_2O	−0.04	0.07
Zn-site	0.80	0.98
Cu-site	−0.02	0.79

of the WT and mutant proteins, the residue D124 donates −0.22e, mostly to the Zn-site. The most direct way for this charge transfer to occur is via the D124−H71 interaction. The formally negative charge of D124 is delocalized, which is expected to result in a stabilization of the aspartate residue.

The natural charges for the WT and H46R models without the H71 residue are given in Table 4. In the WT models, the removal of the H71 residue, which is the link between D124

dx.doi.org/10.1021/ic202416d | Inorg. Chem. 2012, 51, 5561−5568

Table 4. Natural Charges for the Copper-Free Models of the WT-CuZnSOD and Its H46R Mutant, without the H71 Residue

residue or fragment	wild-type (e)	H46R (e)
Zn(II)	1.58	1.59
D124	−0.88	−0.78
H63	0.04	0.05
H80	0.09	0.09
D83	−0.80	−0.79
H48	0.02	0.06
H/R46	−0.08	0.76
H120	0.06	0.01
H_2O	−0.04	0.02
Zn site	0.92	0.94
Cu site	−0.05	0.84

and the zinc center, eliminates the charge transfer from D124 to the zinc site. Since the Cu site cannot accept charge, the negative natural charge in the D124 residue increases. In the H46R mutant models, the charge transfer from D124 to the Zn(II) center is also eliminated by the removal of H71, but the R46 residue is able to accept charge from D124. Because of this, the natural charge on the D124 residue is not altered by the removal of H71.

3.3.2. FopBO Analyses. The bond orders for the D124−H71 and D124−H/R46 interactions were determined by using the first-order perturbation theory bond order indicator (fopBO). The figures showing the results for this analyses are available as Supporting Information. In the complete model, the interactions between D124−H71 and D124−H46 are practically equivalent. Upon removal of H71, the D124−H71 interaction obviously disappears, and the bond order for the D124−H46 interaction increases. However, the increase in the bond order does not compensate the loss of the D124−H71 interaction. The orbital interactions for D124 are thus weakened due to the removal of H71.

In the mutant model, D124 forms two hydrogen bonds to the R46 residue, when H71 is removed. The bond order of these hydrogen bonds almost completely compensate for the loss of the D124−H71 interactions. Thus, when H71 is removed, the D124 residue is less destabilized in the H46R mutant than in the WT model.

The fopBO and NBO analyses show that, for the H46R mutant, the two hydrogen bonds stabilize the reaction product of the dissociation reaction of the H71 residue. These results agree with the calculated energies and partial charges.

3.4. The Metal Site in the H46R-CuZnSOD Crystallographic Structure. In the crystallographic structures the D124 residue is farther away from R46 in the mutant than from H46 in the WT structure. In the mutant structure, the structural element containing the residue D124 appears in a distorted state. The residue D124 is complete in the crystallographic structure, but the structural element to which it belongs lacks from residues L126−G141.[32] It is difficult to conclude, only from the structure, whether the increased distance between residues D124 and R46 causes the damage to the structure of the subsequence L126−G141 or whether it is the other way around. To explore both alternatives, the molecular structures of the reduced models for the metal-binding site of the H46R mutant were optimized at the DFT level using the mutant crystallographic structure as starting geometry.

One of the optimized protein models contained the D125 residue, as well as the backbone of D124 and D125. The other optimized protein model contained the same residues, but the lateral chain of the residue D125 was removed to assess its importance. Considering the distorted structure of the mutant-binding site, the solvent effects were treated with COSMO using a dielectric constant of 20, which is intermediate between the dielectric constant for water (80) and that of 4 for the inside of a folded CuZnSOD.[30] The D124−R46 distances obtained in calculations are compared to crystallographic data in Table 5.

Table 5. Distances (in Å) for the O−N_ε and O−N_η Interactions between D124 and R46 in the Crystallographic Structure for the H46R Mutant of CuZnSOD[32] (Crystal), for a BP86-Optimized Model (DFT), and for a BP86-Optimized Model without the Lateral Chain of the D125 Residue (DFT-D125)

structure	oxygen	ε-nitrogen (Å)	η-nitrogen (Å)
crystal	O_1	3.9	3.2
crystal	O_2	5.8	4.4
DFT-D125	O_1	2.7	3.4
DFT-D125	O_2	4.9	4.9
DFT	O_1	3.8	3.0
DFT	O_2	2.8	3.5

The distances are generally shorter in the optimized structures than in the crystallographic one. In the presence of the D125 lateral chain, the D124−R46 distances are comparable with the D124−H46($N_{\varepsilon 2}$) ones in the crystallographic structures for the WT protein.[11,10] The similar distances suggest that the interaction between the two residues in H46R CuZnSOD is not less favorable than the one between D124 and H46 in the WT protein. Thus, the weakening of the D124−R46 interaction in the mutant crystallographic structure appears to be due to the damaged secondary structure of the sequence between the residues L126 and G141. The damage could be produced by the detachment of H71 from the metal site, since the structural element containing H71 and the one containing the L126−G141 subsequence can be seen to be in spatial contact.[10,11,32]

Table 5 shows that the D124−R46 distances are longer for the structures without the lateral chain of the residue D125, suggesting that one role for this residue is to keep the structural integrity of the zinc site. The negative charge of the D125 residue might also destabilize D124, rendering the removal of H71 from the Zn(II) site less favorable. This suggestion for the role of D125 is in agreement with experimental results showing that mutations of D125 lead to an impaired binding of zinc and copper ions.[23]

4. CONCLUSIONS

The results obtained in the present work suggest that the reduction in the affinity of the residue H71 in the H46R mutant of CuZnSOD is due to the stabilization of the D124 residue by R46 when H71 is absent. The importance of the D124 residue on the structural integrity of the zinc site is known from mutation experiments that show that the damage appears in the zinc site of the D124N and D124V mutants.[8] The exact role of the residue D124 in the zinc site stability was, though, unelucidated. The present results suggest that the role of D124 is to increase the metal site affinity for H71 by destabilizing the

dx.doi.org/10.1021/ic202416d | Inorg. Chem. 2012, 51, 5561−5568

fragment that results from the dissociation of H71. In a recent study, Molnar et al. (2009)[58] found that a common characteristic of all the 15 ALS-linked CuZnSOD mutants they investigated is an increased mobility in the electrostatic loop of the protein, which is the structural element containing D124 and D125. Although the increased mobility was not proven to affect D124 or D125 in all cases, it is reasonable to assume that the arrangement of both residues have to be altered if the structural integrity of the rest of the loop is compromised. Thus, alterations in D124 and D125 like the ones described in this work most likely are common to all ALS-linked CuZnSOD mutations. Our results indicate that perturbations in the D124 residue and probably also in D125 can compromise the integrity of the zinc site. The zinc release from CuZnSOD can cause the effects commonly associated with fALS, including CuZnSOD aggregation. There is evidence suggesting that alterations of zinc homeostasis might be one of, or even the main reason for, CuZnSOD-related fALS syndrome, at least for some of the mutants.[28,29] A previous literature review pointed out that a Zn(II)-homeostasis alteration might lead to all the pathological features commonly associated with ALS.[27] Although the D124-Zn hypothesis must be assessed using other methodologies and by studying other fALS-linked CuZnSOD mutants, the present study gives useful indications for understanding the pathogenic process of CuZnSOD-related fALS and possibly also of ALS in general.

■ ASSOCIATED CONTENT

Supporting Information

Figure 1: Bond orders for the D124−H71 and D124−H46 interactions for the reduced model of the copper-free metal site of WT-CuZnSOD. Figure 2: Bond orders for the D124−H46 interaction for the reduced model of the copper-free metal site of WT-CuZnSOD, without the H71 residue. Figure 3: Bond orders for the D124−H71 and D124−R46 interactions for the reduced model of the copper-free metal site of H46R-CuZnSOD. Bond orders for the D124−R46 interaction for the reduced model of the copper-free metal site of the H46R mutant CuZnSOD, without the H71 residue. This material is available free of charge via the Internet at http://pubs.acs.org.

■ AUTHOR INFORMATION

Corresponding Author

*E-mail: rmera@chem.helsinki.fi.

Notes

The authors declare no competing financial interest.

■ ACKNOWLEDGMENTS

F.M. acknowledges financial support from FONDECYT under Project 1100162 (Conicyt-Chile), Project Millennium P07-006-F, and Basal Financing Program CONICYT-FB0807 (CEDENNA). S.M. and R.M. acknowledge Conicyt-Chile for Ph.D. scholarships. D.S. and R.M acknowledge financial support from the Magnus Ehrnrooth fundation and from The Academy of Finland throught its Centers of Excellence Programme 2006-2011. R.M. ackonwledges the Human Frontier Science Program Organization (HFSPO) for financial support.

■ REFERENCES

(1) Kiernan, M. C.; Vucic, S.; Cheah, B. C.; Turner, M. R.; Eisen, A.; Hardiman, O.; Burrell, J. R.; Zoing, M. C. *Lancet* **2011**, *377*, 942−955.

(2) Miller, R. G.; Mitchell, J. D.; Lyon, M.; Moore, D. H. *Cochrane Database Syst. Rev.* **2007**, CD001447.

(3) Lill, C. M.; Abel, O.; Bertram, L.; Al-Chalabi, A. *Amyotrophic Lateral Scler.* **2011**, *12*, 238−249.

(4) Abel, O. ALS online genetic database. http://alsod.iop.kcl.ac.uk/.

(5) Cleveland, D. W.; Rothstein, J. D. *Nat. Rev. Neurosci.* **2001**, *2*, 806−819.

(6) Seetharaman, S. V.; Prudencio, M.; Karch, C.; Holloway, S. P.; Borchelt, D. R.; Hart, P. J. *Exp. Biol. Med.* **2009**, *234*, 1140−1154.

(7) Crow, J. P.; Sampson, J. B.; Zhuang, Y.; Thompson, J. A.; Beckman, J. S. *J. Neurochem.* **1997**, *69*, 1936−1944.

(8) Banci, L.; Bertini, I.; Cabelli, D. E.; Hallewell, R. A.; Tung, J. W.; Viezzoli, M. S. *Eur. J. Biochem.* **1991**, *196*, 123−128.

(9) Branco, R. J. F.; Fernandez, P. A.; Ramos, M. J. *J. Phys. Chem. B.* **2006**, *110*, 16754−16762.

(10) Hough, M. A.; Hasnain, S. S. *J. Biol. Mol.* **1999**, *287*, 579−592.

(11) Strange, R. W.; Antonyuk, S.; Hough, M. A.; Doucette, P. A.; Valentine, J. S.; Hasnain, S. S. *J. Mol. Biol.* **2006**, *356*, 1152−1162.

(12) Hough, M. A.; Hasnain, S. S. *Structure* **2003**, *11*, 937−946.

(13) Rakhit, R.; Chakrabartty, A. *Biochim. Biophys. Acta* **2006**, *1762*, 1025−1037.

(14) Furukawa, Y.; Torres, A. S.; O'Halloran, T. V. *EMBO J.* **2004**, *23*, 2872−2881.

(15) Outten, C. E.; O'Halloran, T. V. *Science* **2001**, *292*, 2488−2492.

(16) Maret, W.; Li, Y. *Chem. Rev.* **2009**, *109*, 4682−4707.

(17) Colvin, R. A.; Holmes, W. R.; Fontaine, C. P.; Maret, W. *Metallomics* **2010**, *2*, 306−317.

(18) Valentine, J. S.; Hart, P. J. *Proc. Natl. Acad. Sci. U.S.A.* **2003**, *100*, 3617−3622.

(19) Perry, J.; Shin, D.; Getzoff, E.; Tainer, J. *Biochim. Biophys. Acta, BBA* **2010**, *1804*, 245−262.

(20) Roberts, B. R.; Tainer, J. A.; Getzoff, E. D.; Malencik, D. A.; Anderson, S. R.; Bomben, V. C.; Meyers, K. R.; Karplus, P. A.; Beckman, J. S. *J. Mol. Biol.* **2007**, *373*, 877−890.

(21) Kayatekin, C.; Zitzewitz, J. A.; Matthews, C. R. *J. Mol. Biol.* **2008**, *384*, 540−555.

(22) Banci, L.; Bertini, I.; Durazo, A.; Girotto, S.; Gralla, E. B.; Martinelli, M.; Valentine, J. S.; Vieru, M.; Whitelegge, J. P. *Proc. Natl. Acad. Sci. U.S.A.* **2007**, *104*, 11263−7.

(23) Hayward, L. J.; Rodriguez, J. A.; Kim, J. W.; Tiwari, A.; Goto, J. J.; Cabelli, D. E.; Valentine, J. S.; Brown, R. H. *J. Biol. Chem.* **2002**, *277*, 15923−15931.

(24) Elam, J. S.; Taylor, A. B.; Strange, R.; Antonyuk, S.; Doucette, P. A.; Rodriguez, J. A.; Hasnain, S. S.; Hayward, L. J.; Valentine, J. S.; Yeates, T. O.; Hart, P. J. *Nat. Struct. Biol.* **2003**, *10*, 461−467.

(25) Goto, J. J.; Zhu, H.; Sanchez, R. J.; Nersissian, A.; Gralla, E. B.; Valentine, J. S.; Cabelli, D. E. *J. Biol. Chem.* **2000**, *275*, 1007−1014.

(26) Zhang, N.-N.; He, Y.-X.; Li, W.-F.; Teng, Y.-B.; Yu, J.; Chen, Y.; Zhou, C.-Z. *Proteins* **2010**, *78*, 1999−2004.

(27) Smith, A. P.; Lee, N. M. *Amyotrophic Lateral Scler.* **2007**, *8*, 131−143.

(28) Kim, J.; Kim, T.-Y.; Hwang, J. J.; Lee, J.-Y.; Shin, J.-H.; Gwag, B. J.; Koh, J.-Y. *Neurobiol. Dis.* **2009**, *34*, 221−229.

(29) Lelie, H. L.; Liba, A.; Bourassa, M. W.; Chattopadhyay, M.; Chan, P. K.; Gralla, E. B.; Miller, L. M.; Borchelt, D. R.; Valentine, J. S.; Whitelegge, J. P. *J. Biol. Chem.* **2011**, *286*, 2795−2806.

(30) Pelmenschikov, V.; Siegbahn, P. E. M. *Inorg. Chem.* **2005**, *44*, 3311−3320.

(31) Branco, R. J. F.; Fernandez, P. A.; Ramos, M. J. *J. Mol. Struc. THEOCHEM* **2005**, *729*, 141−146.

(32) Antonyuk, S.; Stine, J. A.; Hough, M. A.; Strange, R. W.; Doucette, P. A.; Rodriguez, J. A.; Hayward, L. J.; Valentine, J. S.; Hart, P. J.; Hasnain, S. S. *Protein Sci.* **2005**, *14*, 1201−1213.

(33) Becke, A. D. *Phys. Rev. A* **1988**, *38*, 3098−3100.

(34) Perdew, J. J. *Phys. Rev. B* **1986**, *33*, 8822−8824.

(35) Grimme, S. *J. Comput. Chem.* **2006**, *27*, 1787−1799.

(36) Eichkorn, K.; Treutler, O.; Öhm, H.; Häser, M.; Ahlrichs, R. *Chem. Phys. Lett.* **1995**, *242*, 652−660.

(37) Lee, C.; Yang, W.; Parr, R. G. *Phys. Rev. B* **1988**, *37*, 785−789.

(38) Perdew, J. P.; Wang, Y. *Phys. Rev. B* **1992**, *45*, 13244−13249.
(39) Tao, J.; Perdew, J. P.; Staroverov, V. N.; Scuseria, G. E. *Phys. Rev. Lett.* **2003**, *91*, 146401.
(40) Adamo, C.; Barone, V. *J. Chem. Phys.* **1998**, *108*, 664−675.
(41) Becke, A. D. *J. Chem. Phys.* **1993**, *98*, 5648−5652.
(42) Vosko, S. H.; Wilk, L.; Nusair, M. *Can. J. Phys.* **1980**, *58*, 1200−1211.
(43) Stevens, P. J.; Devlin, F. J.; Chabalowski, C. F.; Frisch, M. J. *J. Phys. Chem.* **1994**, *98*, 11623−11627.
(44) Neese, F.; Wennmohs, F.; Hansen, A.; Becker, U. *Chem. Phys.* **2009**, *356*, 98−109.
(45) Weigend, F.; Ahlrichs, R. *Phys. Chem. Chem. Phys.* **2005**, *7*, 3297−3305.
(46) Neese, F. *WIREs Comput. Mol. Sci* **2012**, *2*, 73−78.
(47) Neese, F. *ORCA − An ab Initio, Density Functional and Semiempirical Program Package*, Version 2.4; Universität Bonn: Germany, 2004.
(48) Klamt, A.; Schüürmann, G. *J. Chem. Soc., Perkin Trans. 2* **1993**, 799−805.
(49) Sinnecker, S.; Rajendran, A.; Klamt, A.; Diedenhofen, M.; Neese, F. *J. Phys. Chem A* **2006**, *110*, 2235−2245.
(50) Glendening, E. D.; Badenhoop, J. K.; Reed, A. E.; Carpenter, J. E.; Bohmann, J. A.; Morales, C. M.; Weinhold, F. *The NBO Program 5.0*; University of Wisconsin: Madison, Wisconsin, 2001.
(51) Weinhold, F. In *Encyclopedia of Computational Chemistry*; Schleyer, P. v. R., Allinger, N. L., Clark, T., Gasteiger, J., Kollman, P. A., Schaefer, H. F., III, Schreiner, P. R., Eds.; John Wiley and Sons: New York, 1998; pp 1792−1811.
(52) Badenhoop., J. K.; Weinhold, F. *J. Chem. Phys.* **1997**, *107*, 5406−5420.
(53) Mera-Adasme, R.; Mendizabal, F.; Olea-Azar, C.; Miranda-Rojas, S.; Fuentealba, P. *J. Phys. Chem. A* **2011**, *115*, 4397−4405.
(54) Sousa, S. F.; Fernandes, P. A.; Ramos, M. J. *J. Am. Chem. Soc.* **2007**, *129*, 1378−1385.
(55) van der Wijst, T.; Fonseca, G., C.; Stewart, M.; Bickelhaupt, F. M. *Chem. Phys. Lett.* **2006**, *426*, 415−421.
(56) Amin, E. A.; Truhlar, D. G. *J. Chem. Theory Comput.* **2008**, *4*, 75−85.
(57) Antony, J.; Grimme, S. *Phys. Chem. Chem. Phys.* **2006**, *8*, 5287−5293.
(58) Molnar, K. S.; Karabacak, N. M.; Johnson, J. L.; Wang, Q.; Tiwari, A.; Hayward, L. J.; Coales, S. J.; Hamuro, Y.; Agar, J. N. *J. Biol. Chem.* **2009**, *284*, 30965−30973.